International Journal of
Mathematical Modelling & Computations
Vol. 07, No. 01, Spring 2015, 55- 65

Influence of an External Magnetic Field on the Peristaltic Flow of a Couple Stress Model of Blood Flow Through a Porous Medium

A. Ahmad Dar [a,*] and K. Elangovan [b]

[a] *Department of Mathematics, Annamalai University, Annamalainagar Tamil Nadu, India*,
[b] *Mathematics Section FEAT, Annamalai University, Annamalainagar Tamil Nadu, India*.

Abstract. Magnetohydrodynamic(MHD) peristaltic flow of a Couple Stress model of blood flow through a permeable channel is examined in this investigation. The flow analysis is performed in the presence of an External Magnetic Field. Long wavelength and low Reynolds number methodology is actualized. Mathematical expressions of axial velocity, pressure gradient and volume flow rate are obtained. Pressure rise, frictional force and pumping phenomenon are portrayed and symbolized graphically. The elemental characteristics of this analysis is a complete interpretation of the influence of Couple Stress Parameter, magnetic number, non dimensional amplitude ratio and permeability parameter on the velocity, pressure gradient, pressure rise and frictional forces.

Received: 12 August 2016, Revised: 28 December 2016, Accepted: 26 February 2017.

Keywords: Peristalsis, Couple Stress fluid, MHD flow, Reynold's number, Pressure gradient.

Index to information contained in this paper

1. Introduction

Peristalsis is a form of transporting fluids in which an induced wave causes the propagation of the flexible walls of a channel/tube. This mechanism is found in many physiological situations like urine transport from kidney to the bladder through the ureter, swallowing of food through the esophagus, movement of chyme in the gastrointestinal tract, transport of spermatozoa in the ducts efferent of the male

*Corresponding author. Email: darsalik88@gmail.com.

reproductive organ, movement of ovum in the female fallopian tube, vasomotion of small blood vessels, motion of spermatozoa in cervical canal, transport of bile in bile duct. Some worms like earth-worm use peristalsis for their locomotion.Some biomedical instruments such as heart-lung machine work on this principle. Mechanical devices like finger pumps, roller pumps use peristalsis to pump blood, slurries and corrosive fluids. The mechanism of peristaltic transport has been exploited for industrial applications like sanitary fluid transport, transport of corrosive fluids where the contact of the fluid with the machinery parts is prohibited and transport of a toxic liquid is used in nuclear industry to avoid contamination from the outside environment.

Various studies on peristaltic transport, experimental as well as theoretical, have been carried out by many researchers to explain peristaltic pumping in physiological systems. Srivastava et al. [21] studied the peristaltic transport of a physiological fluid: part I flow in non-uniform geometry. Latham [5] investigated the fluid mechanics of peristaltic pump. Very recently, Mekheimer [9] has discussed the effects of the induced magnetic field on peristaltic flow of a couple stress fluid in a slit channel. According to him, the magnetohydrodynamic flow of a fluid in channel in connection with peristaltic flow has applications in physiological fluids. Recently, Sinha et al.[17] modeled peristaltic transport of MHD flow and heat transfer in an asymmetric channel. Srinivasacharya et al.[19] investigated peristaltic flow of micropolar fluid through a tube under low Reynolds number and long wavelength approximations. They found that pumping improves for micropolar fluids compared with Newtonian fluids. Hayat et al.[4] investigated the effects of different wave forms on peristaltic flow of micropolar fluids through a channel and reported that the maximum pressure against which peristalsis works, increases with the coupling number but decreases with the micropolar parameter. Rathod and Mahadev [12] studied slip effects and heat transfer on MHD peristaltic flow of Jeffrey fluid in an inclined channel. Rathod and Laxmi [11] studied peristaltic transport of a conducting fluid in an asymmetric vertical channel with heat and mass transfer. Pandey and Chaube [10] studied peristaltic flow of a micropolar fluid through a porous medium in the presence of an external magnetic.

Flow through porous media has been of considerable interest in the recent years due to the potential application in all fields of Engineering, Geo-fluid dynamics and Bio-Mechanics. For example study of flow through porous media is immense use to understand transport process in lungs, in kidneys, gallbladder with stones, movement of small blood vessels and tissues cartilage and bones etc. Most of the tissues in the body (e.g. bone, cartilage, muscle) are deformable porous media. Sobh [18] investigated peristaltic transport of a magneto Newtonian fluid through a porous medium. Recently, Abd-Alla et al.[1], Tripathi [23], Mekheimer et al.[7], Maiti and Misra [6], Elshehawey et al.[3] studied the interaction of peristalsis through a porous medium. The peristaltic fluid flow through channels with flexible walls has been studied by RaviKumar et al.[14]-[16]. Vajravelu et al.[24] discussed the peristaltic flow and heat transfer in a vertical porous annulus, with long wave approximation.

The couple stress fluid is a special case of the non-Newtonian fluids where these fluids are consisting of rigid randomly oriented particles suspended in a viscous medium and their sizes are taken into account. There have only few attempts for studying the peristaltic flow of a couple stress fluids, first discussed by Stokes [22]. For couple stress fluids, there have been a number of studies carried out due to its widespread industrial and scientific applications, such as the works of Srivastava [20], Mekheimer and Abd elmaboud [8] and Sobh [25]. Ajaz and Elangovan [2] studied the influence of an inclined magnetic field on Heat and Mass transfer of the peristaltic flow of a couple stress fluid in an inclined channel.

2. Mathematical Formulation

Consider the flow of an incompressible, electrically conducting Couple stress fluid through a porous medium in presence of an external magnetic field. The fluid fills a two dimensional channel of non uniform thickness. Sinusoidal waves of constant speed (c) propagate along the channel boundaries. The plates of the channel are assumed to be electrically insulated. We choose a rectangular coordinate system for the channel with x along center-line in the direction of wave propagation and y transverse to it.
The geometry of the channel walls is given by

$$h'(X',t') = a(x') + b\sin\frac{2\pi}{\lambda}(X' - ct') \tag{1}$$

with

$$a(x') = a + kx' \tag{2}$$

Where $a(x')$ is the half width of the channel at any axial distance x' from inlet, a is the half-width at the inlet, b is the amplitude, $k(<< 1)$ is a constant whose magnitude depends on the length of the channel and exit and inlet dimensions, λ is the wavelength, c is the wave speed, and t' is the time.

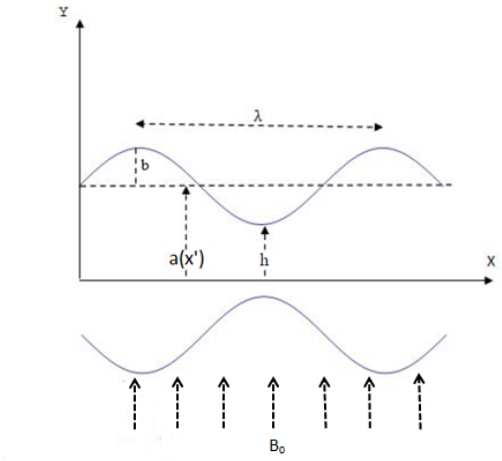

Figure 1. The Geometry of the problem

The flow is unsteady in the laboratory frame (X', Y') whereas it is steady if observed in the coordinate system (x', y'), termed as a wave frame, moving with velocity c. The transformation from the fixed frame of reference (X', Y') to the wave frame of reference (x', y') is given by

$$x' = X' - ct', y' = Y', u' = U' - c, v' = V'. \tag{3}$$

In absence of body forces and body couple, the governing equations for the flow in wave frame of reference are given by

$$\frac{\partial u'}{\partial x'} + \frac{\partial v'}{\partial y'} = 0 \tag{4}$$

$$\rho\left(u'\frac{\partial u'}{\partial x'}+v'\frac{\partial u'}{\partial y'}\right)=-\frac{\partial p'}{\partial x'}+\mu\left(\frac{\partial^2 u'}{\partial x'^2}+\frac{\partial^2 u'}{\partial y'^2}\right)-\eta^*\left(\frac{\partial^4 u'}{\partial x'^4}+\frac{\partial^4 u'}{\partial y'^4}+2\frac{\partial^4 u'}{\partial x'^2\partial y'^2}\right)$$
$$-\sigma B_0^2(u'+c)-\frac{\mu}{K_1'}(u'+c) \tag{5}$$

$$\rho\left(u'\frac{\partial v'}{\partial x'}+v'\frac{\partial v'}{\partial y'}\right)=-\frac{\partial p'}{\partial y'}+\mu\left(\frac{\partial^2 v'}{\partial x'^2}+\frac{\partial^2 v'}{\partial y'^2}\right)-\eta^*\left(\frac{\partial^4 v'}{\partial x'^4}+\frac{\partial^4 v'}{\partial y'^4}+2\frac{\partial^4 v'}{\partial x'^2\partial y'^2}\right)$$
$$-\frac{\mu}{K_1'}v' \tag{6}$$

where u' and v' are the velocity components in the x' and y' directions, respectively, ρ is the density of the fluid, p' is the pressure, μ is the viscosity constant of the classical fluid dynamics, η^* is the coefficient of couple stress, $\sigma$is the electrical conductivity, B_0 is the strength of the magnetic field and K_1' is the permeability of the porous medium.

Now we introduce the non-dimensional variables and parameters as follows

$$x=\frac{x'}{\lambda},y=\frac{y'}{a},u=\frac{u'}{c},v=\frac{v'}{\delta c},\delta=\frac{a}{\lambda},t=\frac{ct'}{\lambda},p=\frac{p'a^2}{c\lambda\mu},K_1=\frac{K_1'}{a^2},h=\frac{h'}{a},$$
$$M=\sqrt{\frac{\sigma}{\mu}}aB_0,\ R_e=\frac{\rho ca}{\mu},S=\frac{\eta^*}{\mu a^2},h=1+\frac{\lambda kx}{a}+\phi\sin[2\pi(x-t)],\phi=\frac{b}{a} \tag{7}$$

Where, M is termed as the Hartman number, Re as the Reynolds number and δ as the wave number.

Using the non-dimensional variables and parameters given above in Eqs.(5) and (6), we get the modified equations as

$$R_e\delta\left(u\frac{\partial u}{\partial x}+v\frac{\partial u}{\partial y}\right)=-\frac{\partial p}{\partial x}+\left(\delta^2\frac{\partial^2 u}{\partial x^2}+\frac{\partial^2 u}{\partial y^2}\right)$$
$$-S\left(\delta^4\frac{\partial^4 u}{\partial x^4}+\frac{\partial^4 u}{\partial y^4}+2\delta^2\frac{\partial^4 u}{\partial x^2\partial y^2}\right)-M^2(u+1)-\frac{1}{K_1}(u+1) \tag{8}$$

$$R_e\delta^3\left(u\frac{\partial v}{\partial x}+v\frac{\partial v}{\partial y}\right)=-\frac{\partial p}{\partial y}+\delta^2\left(\delta^2\frac{\partial^2 u}{\partial x^2}+\frac{\partial^2 u}{\partial y^2}\right)$$
$$-S\delta^2\left(\delta^4\frac{\partial^4 v}{\partial x^4}+\frac{\partial^4 v}{\partial y^4}+2\delta^2\frac{\partial^4 u}{\partial x^2\partial y^2}\right)-\delta^2\frac{v}{K_1} \tag{9}$$

Using the long wavelength approximation and neglecting the wave number along with low Reynolds number, one can find from Eqs. (8) and (9) that

$$-\frac{\partial p}{\partial x}+\frac{\partial^2 u}{\partial y^2}-S\frac{\partial^4 u}{\partial y^4}-M^2(u+1)-\frac{1}{K_1}(u+1)=0 \tag{10}$$

$$\frac{\partial p}{\partial y}=0 \tag{11}$$

Since it is presumed that the couple stress is caused by the presence of the suspending particles, obviously the clear fluid cannot support couple stress at the boundary, hence we have tactically assumed that the components of the couple stress tensor vanish at the wall, the corresponding boundary conditions in dimensionless form are given by

$$\frac{\partial u}{\partial y} = 0 \quad \frac{\partial^3 u}{\partial y^3} = 0 \quad at \;\; y = 0 \tag{12}$$

$$u = 0 \quad \frac{\partial^2 u}{\partial y^2} = 0 \quad at \;\; y = h(x,t) = 1 + \frac{\lambda k x}{a_0} + \phi \sin 2\pi(x - ct) \tag{13}$$

3. Method of Solution

Solving Eq. (10) by using the boundary conditions from Eqs. (12) and (13), we get

$$u = -\frac{A}{\left(\frac{1}{K_1} + M^2\right)(C_1^2 - C_2^2)} \left[C_2^2 \frac{\cosh[C_1 y]}{\cosh[C_1 h]} - C_1^2 \frac{\cosh[C_2 y]}{\cosh[C_2 h]} + (C_1^2 - C_2^2)\right] \tag{14}$$

Where $C_1 = \sqrt{\frac{1-\sqrt{1-4S(\frac{1}{K_1}+M^2)}}{2S}}$, $C_2 = \sqrt{\frac{1+\sqrt{1-4S(\frac{1}{K_1}+M^2)}}{2S}}$, $A = \frac{1}{K_1} + M^2 + \frac{dp}{dx}$.

The Volume flow rate in the fixed frame is given by

$$Q(X', t') = \int_0^{h'} U'(X', Y', t') dY', \tag{15}$$

where h' is a function of X' and t'.

The rate of volume flow in the wave frame can be expressed as

$$q'(x') = \int_0^{h'} u'(x', y') dy', \tag{16}$$

where h' is a function of x' alone. Eqs. (3), (15) and (16) yield

$$Q(X', t') = q'(x') + ch'(X', t'). \tag{17}$$

The time averaged mean flow rate over a period T at a fixed position X' is expressed as

$$Q'(X') = \frac{1}{T} \int_0^T Q(X', t') dt'. \tag{18}$$

Using Eq. (17) into Eq. (18), we get

$$Q'(X') = q'(x') + ac \tag{19}$$

The dimensionless mean flow rates $\widetilde{Q}$ (in the laboratory frame) and q (in the wave frame) are defined as

$$\widetilde{Q}(X) = \frac{Q'(X')}{ac}, \qquad q(x) = \frac{q'(x')}{ac} \tag{20}$$

By using Eq. (20) in Eq. (19), we get

$$\widetilde{Q} = q + 1 \tag{21}$$

where

$$q(x) = \int_0^h u(x,y)dy. \tag{22}$$

Substitute Eq. (14) in Eq. (22), we have

$$q = -\frac{\left(\frac{1}{K_1} + M^2 + \frac{dp}{dx}\right)}{\left(\frac{1}{K_1} + M^2\right)(C_1^2 - C_2^2)}\left[\frac{C_2^2}{C_1}\tanh(C_1h) - \frac{C_1^2}{C_2}\tanh(C_2h) + (C_1^2 - C_2^2)h\right] \tag{23}$$

The pressure gradient obtained from Eq. (23) and Eq. (21) can be expressed as

$$\frac{dp}{dx} = -\left[\frac{(\frac{1}{K_1}+M^2)(C_1C_2)(C_1^2-C_2^2)(\widetilde{Q}-1)}{C_2^3\tanh(C_1h)-C_1^3\tanh(C_2h)+(C_1C_2)(C_1^2-C_2^2)h}\right] - \left(\frac{1}{K_1} + M^2\right) \tag{24}$$

The expressions for pressure rise Δp and the frictional force F over one wavelength are given by

$$\Delta p = \int_0^1 \left(\frac{dp}{dx}\right) dx \tag{25}$$

$$F = \int_0^1 h\left(-\frac{dp}{dx}\right) dx \tag{26}$$

4. Numerical Results and Discussion

In this section, the numerical and the computational results are discussed through the graphical illustration. We have presented the graphical results of the solutions of axial velocity (u), pressure gradient ($\frac{dp}{dx}$), pressure rise (Δp) and friction force (F) for different values of Couple stress (S), Porous medium (K_1), amplitude ratio ϕ and Magnetic number (M).

The axial velocity is shown in the Figs. (2) to (7) for different values of Couple stress parameter (S), Porous parameter (K_1), Magnetic number (M) and amplitude ratio ϕ . Fig. (2) reveals that the axial velocity distribution decreases by increasing the couple stress parameter (S) with $K_1 = 10$. Fig. (3) reveals that the axial velocity distribution increases by increasing the porous parameter (K_1) with $S = 0.1$ and interestingly there is no significant effect of porous parameter (K_1) on the axial velocity (u) for large values of K_1.

The effect of Magnetic field on the axial velocity has been shown in the figs. (4) to (6). These figures illustrate that by increasing the magnetic number (M), the axial velocity decreases with $S \geqslant 0.1$. Fig. (7) illustrates that the axial velocity distribution decreases by increasing the amplitude ratio ϕ.

Figs. (8) to (15) illustrate the variation of pressure gradient $\frac{dp}{dx}$ for a given wavelength versus x, where $x \in [0, 1]$. Fig. (8) shows the variation of $\frac{dp}{dx}$ for variation of the Couple stress parameter S with $t = 0$. We observed that the flow cannot pass easily through the narrow part of the channel i.e $x \in (0.5, 0.9)$. Therefore, it requires large pressure gradient to maintain the same flux to pass it in the narrow part of the channel. Whereas, the flow can easily pass through the wider part of the channel $x \in (0.9, 1)$ without applying the large pressure gradient. It can be seen that an increase in the Couple stress parameter S increases $\frac{dp}{dx}$ in the narrow part of the channel $x \in (0.5, 0.9)$ while in the wider part of the channel $x \in (0, 0.4) \cup (0.9, 1)$ there is no noticeable difference.

Fig. (9) reveals the variation of $\frac{dp}{dx}$ for different values of Couple stress parameter S with $t = 0.5$. We notice that $\frac{dp}{dx}$ is maximum at x=0.2. It is observed that in the narrow part of the channel $x \in (0.1, 0.4)$ it requires large pressure gradient to make the flow as normal fluid flow while in the wider part of the channel $x \in (0, 0.1) \cup (0.4, 1)$ fluid can pass easily because of the low pressure gradient. Fig. (10) reveals the variation of $\frac{dp}{dx}$ for different values of Couple stress parameter S with $t = 0.75$. We notice that $\frac{dp}{dx}$ is maximum at x=0.5. It is observed that in the narrow part of the channel $x \in (0.3, 0.6)$ it requires large pressure gradient to make the flow as normal fluid flow while in the wider part of the channel $x \in (0, 0.3) \cup (0.6, 1)$ fluid can pass easily because of the low pressure gradient. Fig. (11) illustrates the variation of $\frac{dp}{dx}$ for variation of Averaged Flow Rate $\widetilde{Q}$. It is interesting to note that $\frac{dp}{dx}$ decreases with increase in the Averaged flow rate $\widetilde{Q}$. Fig. (12) depicts that by increasing $\phi, \frac{dp}{dx}$ increases in the narrow part of the channel while $\frac{dp}{dx}$ negligibly decreases in the wider part of the channel.

The effect of magnetic field on pressure gradient has been shown in Figs. (13) to (15). On increasing the magnetic number M, $\frac{dp}{dx}$ decreases in the wider part of the channel $x \in (0, 0.4) \cup (0.9, 1)$ while in the narrow part of the channel $x \in (0.5, 0.9)$ there is a negligible decrease in the pressure gradient. The Variation of Pressure

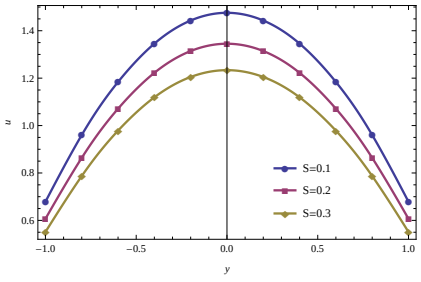

Figure 2. Distribution of axial velocity for different value of S with fixed $K_1 = 10$, $\frac{dp}{dx} = -2$, $\phi = 0.7$, $x = t = \frac{\pi}{4}$, $M = 0.2$, $\lambda = 10$, $k = 0.0005$, $a_0 = 0.01$

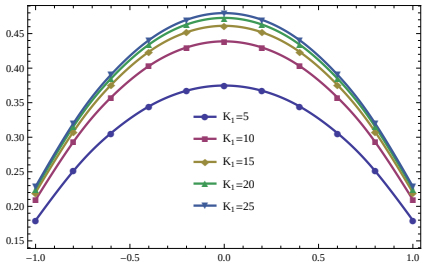

Figure 3. Distribution of axial velocity for different value of K_1 with fixed $S = 0.1$, $M = 1$, $\frac{dp}{dx} = -2$, $x = t = \frac{\pi}{4}$, $\phi = 0.7$, $\lambda = 10$, $k = 0.0005$, $a_0 = 0.01$

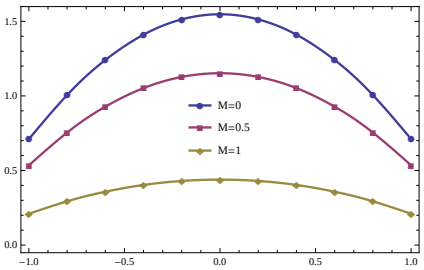

Figure 4. Distribution of axial velocity for different value of M with fixed $S = 0.1$, $K_1 = 10$, $\frac{dp}{dx} = -2$, $\phi = 0.7$, $x = t = \frac{\pi}{4}$, $\lambda = 10$, $k = 0.0005$, $a_0 = 0.01$

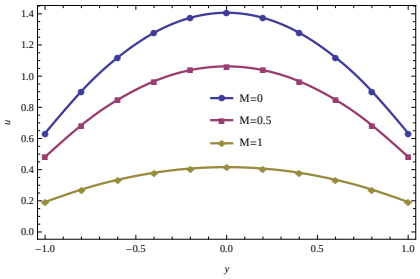

Figure 5. Distribution of axial velocity for different value of M with fixed $S = 0.2$, $K_1 = 10$, $\frac{dp}{dx} = -2$, $\phi = 0.7$, $x = t = \frac{\pi}{4}$, $\lambda = 10$, $k = 0.0005$, $a_0 = 0.01$

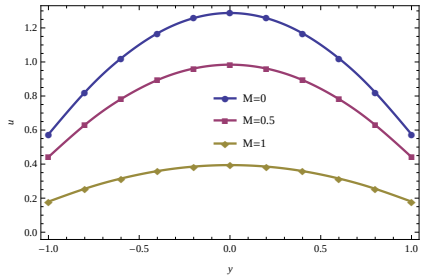

Figure 6. Distribution of axial velocity for different value of M with fixed $S = 0.3$, $K_1 = 10$, $\frac{dp}{dx} = -2$, $\phi = 0.7$, $x = t = \frac{\pi}{4}$, $\lambda = 10$, $k = 0.0005$, $a_0 = 0.01$

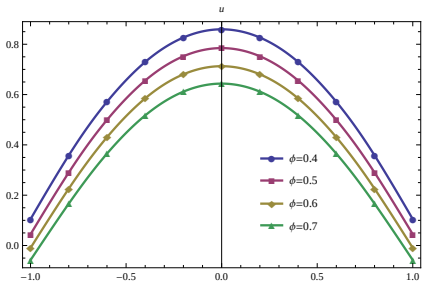

Figure 7. Distribution of axial velocity for different value of ϕ with fixed $S = 0.1$, $K_1 = 10$, $\frac{dp}{dx} = -2$, $x = 0.5, t = \frac{\pi}{2}$, $M = 0.2$, $\lambda = 10$, $k = 0.0005$, $a_0 = 0.01$

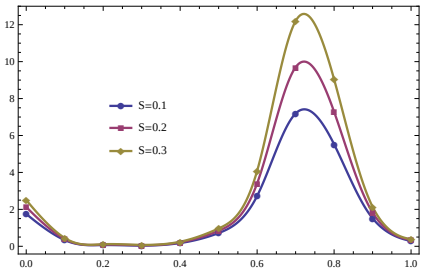

Figure 8. Distribution of axial pressure gradient for different value of S with fixed $K_1 = 10$, $t = 0$, $\phi = 0.7$, $M = 0.5$, $\lambda = 10$, $k = 0.0005$, $a_0 = 0.01$, $\widetilde{Q} = 0.5$.

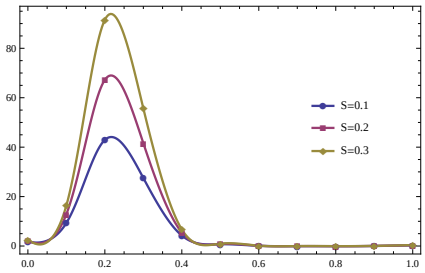

Figure 9. Distribution of axial pressure gradient for different value of S with fixed $K_1 = 10$, $t = 0.5$, $\phi = 0.7$, $M = 0.5$, $\lambda = 10$, $k = 0.0005$, $a_0 = 0.01$, $\widetilde{Q} = 0.5$.

rise Δp over one wavelength, friction force F across one wavelength against the average volume flux $\widetilde{Q}$ has been illustrated in Figs. (16) to (23) for different values of Couple stress parameter S, Porous parameter K_1, amplitude ratio ϕ and magnetic number M. The pressure rise against the volume flow rate for various parameters of interest is illustrated in Figs. (16) to (19). We discern that the pressure rise and volume flow rate have an opposite behavior. In these figures the region is divided into four parts: peristaltic pumping region ($\Delta p > 0, \widetilde{Q} > 0$), retrograde pumping region ($\Delta p > 0, \widetilde{Q} < 0$), augmented region ($\Delta p < 0, \widetilde{Q} > 0$) and free pumping region ($\Delta p = 0$). The region in which $\Delta p > 0, \widetilde{Q} > 0$) is known as the peristaltic pumping region. In this region the peristaltic wave overcomes the pressure rise and induces the fluid in the direction of its propagation. The region where $\Delta p > 0$ and $\widetilde{Q} < 0$ is called a retrograde pumping region. In this region, the flow is opposite to the direction of the peristaltic motion. The region in which $\Delta p < 0, \widetilde{Q} > 0$ is known as augmented pumping region or co-pumping region. In this region, the negative pressure rise increases the flow due to the peristalsis of the walls. In the free pumping region, where $\Delta p = 0$, the fluid is exclusively propelled by the peristalsis of the walls.

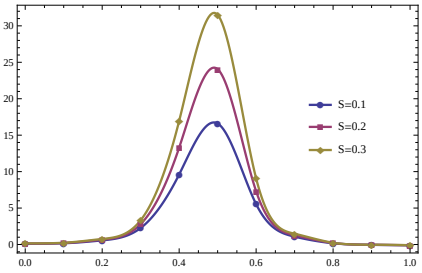

Figure 10. Distribution of axial pressure gradient for different value of S with fixed $K_1 = 10$, $t = 0.75$, $\phi = 0.7$, $M = 0.2$, $\lambda = 10$, $k = 0.0005$, $a_0 = 0.01$, $\widetilde{Q} = 0.5$.

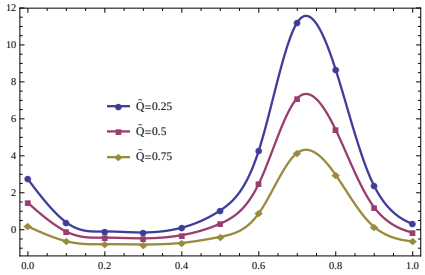

Figure 11. Distribution of axial pressure gradient for different value of $\widetilde{Q}$ with fixed $K_1 = 10$, $t = 0$, $\phi = 0.7$, $\lambda = 10$, $k = 0.0005$, $a_0 = 0.01$, $S = 0.1$.

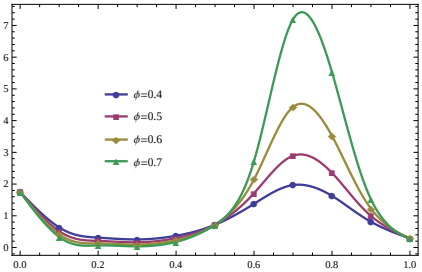

Figure 12. Distribution of axial pressure gradient for different value of ϕ with fixed $K_1 = 10$, $\widetilde{Q} = 0.5$, $t = 0$, $\lambda = 10$, $k = 0.0005$, $M = 0.5$, $a_0 = 0.01$, $S = 0.1$.

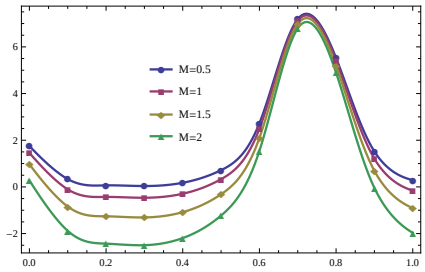

Figure 13. Distribution of axial pressure gradient for different value of M with fixed $K_1 = 10$, $S = 0.1$,$t = 0$, $\phi = 0.7$, $\lambda = 10$, $k = 0.0005$, $a_0 = 0.01$, $\widetilde{Q} = 0.5$.

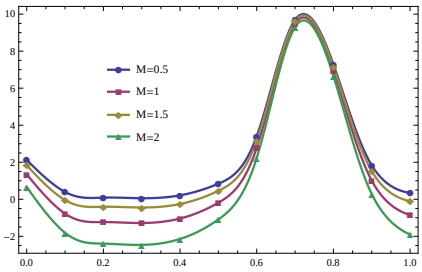

Figure 14. Distribution of axial pressure gradient for different value of M with fixed $K_1 = 10$, $S = 0.2$,$t = 0$, $\phi = 0.7$, $\lambda = 10$, $k = 0.0005$, $a_0 = 0.01$, $\widetilde{Q} = 0.5$.

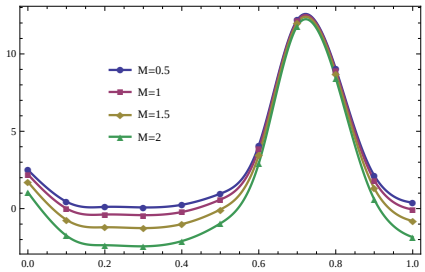

Figure 15. Distribution of axial pressure gradient for different value of M with fixed $K_1 = 10$, $S = 0.3$,$t = 0$, $\phi = 0.7$, $\lambda = 10$, $k = 0.0005$, $a_0 = 0.01$, $\widetilde{Q} = 0.5$.

From Fig. (16), it is depicted that increase of couple stress fluid parameter decreases the pumping rate $\widetilde{Q}$ in the augmented pumping region. In the free pumping region, the pumping rate reaches to a critical value of $\widetilde{Q}$. In the peristaltic and retrograde pumping regions, the pumping rate increases by increasing S. The behavior is quite opposite with increase in amplitude ratio ϕ as shown in Fig. (18). From Fig. (17) it is noticed that on increasing the porous parameter K_1, the pumping rate increases in the augmented, peristaltic and free pumping regions and decreases in the retrograde pumping region. Fig. (19) demonstrates that increase of magnetic effects decreases the pumping rate in the augmented, free and peristaltic pumping regions and increases the pumping rate in the retrograde pumping region.

Figs. (20) to (23) describes the variation of frictional forces F against the flow rate for different parameters of interest. The frictional forces exactly have an opposite behavior when compared to the pressure rise.

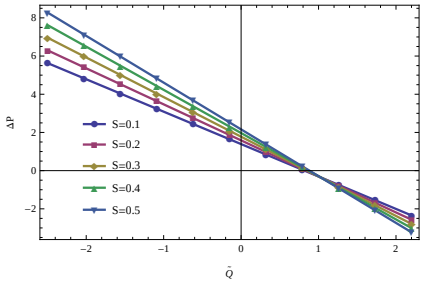

Figure 16. Effect of S on Δp when $K_1 = 10$, $t = \frac{\pi}{4}$, $M = 0.5$, $x = 0.25$, $\phi = 0.7$, $\lambda = 10$, $k = 0.0005$, $a_0 = 0.01$.

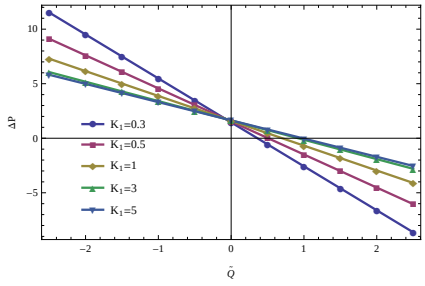

Figure 17. Effect of K_1 on Δp when $S = 0.1$, $t = \frac{\pi}{4}$, $M = 0.5$, $x = 0.25$, $\phi = 0.7$, $\lambda = 10$, $k = 0.0005$, $a_0 = 0.01$.

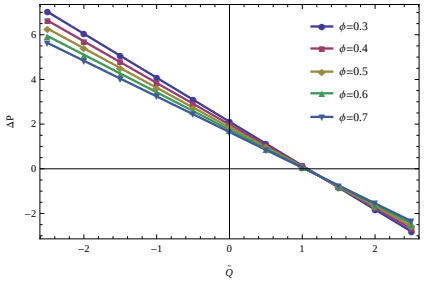

Figure 18. Effect of ϕ on Δp when $S = 0.1$, $t = \frac{\pi}{4}$, $M = 0.5$, $x = 0.25$, $K_1 = 10$, $\lambda = 10$, $k = 0.0005$, $a_0 = 0.01$.

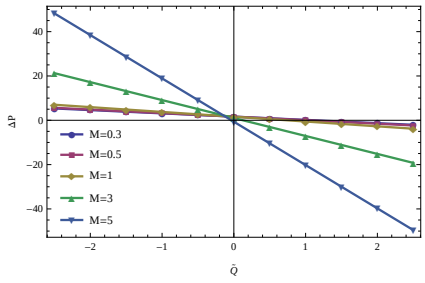

Figure 19. Effect of M on Δp when $S = 0.1$, $t = \frac{\pi}{4}$, $K_1 = 10$, $x = 0.25$, $\phi = 0.7$, $\lambda = 10$, $k = 0.0005$, $a_0 = 0.01$.

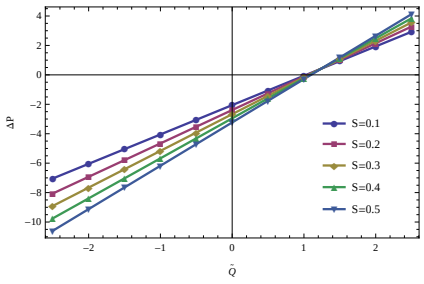

Figure 20. Effect of S on F when $K_1 = 10$, $t = \frac{\pi}{4}$, $M = 0.5$, $x = 0.25$, $\phi = 0.7$, $\lambda = 10$, $k = 0.0005$, $a_0 = 0.01$.

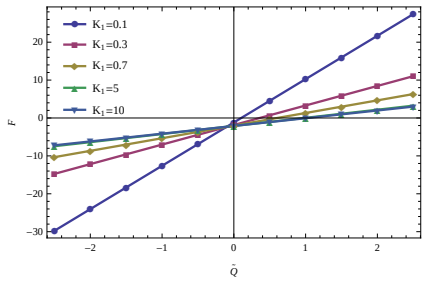

Figure 21. Effect of K_1 on F when $S = 0.1$, $t = \frac{\pi}{4}$, $M = 0.5$, $x = 0.25$, $\phi = 0.7$, $\lambda = 10$, $k = 0.0005$, $a_0 = 0.01$.

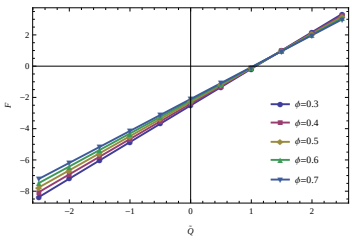

Figure 22. Effect of ϕ on F when $S = 0.1$, $t = \frac{\pi}{4}$, $M = 0.5$, $x = 0.25$, $K_1 = 10$, $\lambda = 10$, $k = 0.0005$, $a_0 = 0.01$.

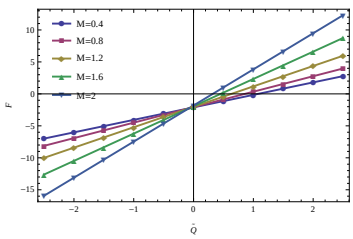

Figure 23. Effect of M on Δp when $S = 0.1$, $t = \frac{\pi}{4}$, $K_1 = 10$, $x = 0.25$, $\phi = 0.7$, $\lambda = 10$, $k = 0.0005$, $a_0 = 0.01$.

5. Conclusions

- Axial velocity increases by increasing K_1 and decreases by increasing the couple stress fluid parameter S, magnetic number M and amplitude ratio ϕ.
- Pressure gradient increases by increasing S and ϕ in the narrow part of the channel while in the wider part of the channel there is no appreciable difference. Magnetic field shows opposite behavior as compared to S.
- By increasing the averaged flow rate $\widetilde{Q}$, $\frac{dp}{dx}$ decreases.
- Best pumping can be seen at higher values of the magnetic field.

- The frictional forces have an opposite behavior as compared to the pressure rise.

References

[1] A. M. Abd-Alla, S. M. Abo-Dahab and R. D. Al-Simery, *Effect of rotation on peristaltic flow of a micropolar fluid through a porous medium with an external magnetic field*, Journal of magnetism and Magnetic materials, **348** (2013) 33-43.

[2] A. Ahmad Dar and K. Elangovan, *Influence of an inclined magnetic field on Heat and Mass transfer of the peristaltic flow of a couple stress fluid in an inclined channel*, World Journal of Engineering, **14 (1)** (2017).

[3] E. F. Elshehawey, N. T. Eldabe, E. M. Elghazy and A. Ebaid, *Peristaltic transport in an asymmetric channel through a porous medium*, Applied Mathematics and computation, **182** (2006) 140-150.

[4] T. Hayat, N. Ali and Z. Abbas, *Peristaltic flow of a micropolar fluid in channel with different wave forms*, Phys Lett. A, **370** (2007) 331-344.

[5] T. W. Latham, *Fluid motion in a peristaltic pump*, M.Sc. Thesis, MIT, Cambridge MA, (1966).

[6] S. Maiti and J. C. Misra, *Peristaltic flow of a fluid in a porous channel: A study having relevance to flow of bile within ducts in a pathological state*, International journal of Engineering Science, **49** (2011) 950-966.

[7] Kh. S. Mekheimer, A. M. Salem and A. Z. Zaher, *Peristaltically induced MHD slip flow in a porous medium due to a surface acoustic wavy medium*, Journal of the Egyptian Mathematical Society, **22** (2014) 143-151.

[8] Kh. S. Mekheimer and Y. Abd elmaboud, *Peristaltic flow of a couple stress fluid in an annulus: Application of an endoscope*, Physica A, **387** (2008) 2403-2415.

[9] Kh. S. Mekheimer, *Effect of induced magnetic field on peristaltic flow of a couple stress fluid*, Phys. Lett. A, **372** (2008) 4271-4278.

[10] S. K. Pandey and M. K. Chaube, *Peristaltic flow of a micropolar fluid through a porous medium in the presence of an external magnetic field*, Communications in Nonlinear Science and Numerical Simulations, **16** (2011) 3591-3601.

[11] V. P. Rathod and D. Laxmi, *Peristaltic Transport of a Conducting Fluid in an Asymmetric Vertical Channel with Heat and Mass Transfer*, Journal of Chemical, Biological and Physical Sci, **4(2)** (2014) 1452-1470.

[12] V. P. Rathod and M. Mahadev, *Peristaltic flow of a Jeffery fluid with slip effects in an inclined channel*, Journal of Chemical, Biological and Physical Sci, **2** (2012) 1987-1997.

[13] S. Ravikumar and R. Siva Prasad, Interaction of Pulsatile flow on the peristaltic motion of couple stress fluid through porous medium in a flexible channel, Eur. J. Pure Appl. Math, **3** (2010) 213-226.

[14] S. Ravikumar, G. Prabhakara Rao and R. Siva Prasad, *Peristaltic flow of a couple stress fluid flows in a flexible channel under an oscillatory flux*, Int. J. of Appl. Math and Mech, **6(13)** (2010) 58-71.

[15] S. Ravikumar, *Peristaltic transportation with effect of magnetic field in a flexible channel under an oscillatory flux*, Journal of Global Research in Mathematical Archives, **1(5)** (2013) 53-62.

[16] S. Ravikumar, *Hydromagnetic Peristaltic Flow of Blood with Channel: A Theoretical Study*, International Journal of Engineering Sciences and Research Technology, **2(10)** (2013) 2863-2871.

[17] A. Sinha, G. C. Shit and N. K. Ranjit, *Peristaltic transport of MHD flow and heat transfer in an asymmetric channel: Effects of variable viscosity, velocity-slip and temperature jump*, Alexandria Engineering Journal, **54** (2015) 691-704.

[18] A. M. Sobh, *Peristaltic transport of a magneto Newtonian fluid through a porous medium*, Turkish Journal of Islamia University of Gaza, **12** (2004) 37-49.

[19] D. Srinivasacharya, M. Mishra and A. R. Rao, *Peristaltic transport of a micropolar fluid in a tube*, Acta Mech, **161** (2003) 165-178.

[20] L. M. Srivastava, *Peristaltic transport of a couple-stress fluid*, Rheologica Acta, **25** (1986) 638-641.

[21] L. M. Srivastava, V. P. Srivastava and S. N. Sinha, *Peristaltic transport of a physiological fluid: Part I Flow in non-uniform geometry*, Biorheol, **20** (1983) 153-166.

[22] V. K. Stokes, *Couple stresses in fluids*, Phys. Fluids, **9** (1966) 1709-1715.

[23] D. Tripathi, *Study of transient peristaltic heat flow through a finite porous channel*, Mathematical and Computer modeling, **57** (2013) 1270-1283.

[24] K. Vajravelu, G. Radhakrishnamacharya and V. Radha Krishnamurthy, *Peristaltic flow heat transfer in a vertical porous annulus with long wave approximation*, Int. J Non-Linear Mech, **42** (2007) 754-759.

[25] A. M. Sobh, *Interaction of Couple Stresses and Slip Flow on Peristaltic Transport in Uniform and Nonuniform Channels*, Turkish J. Eng. Env. Sci, **32** (2008) 117-123.